IMAGE-BASED 3D SURFACE RECONSTRUCTION OF COLD-FORMED STEEL C-SECTIONS

Burcu Güldür Erkal

Hacettepe University, Ankara, Turkey

Abstract

The use of cold-formed steel (CFS) members in construction have increased significantly due to the recent advances in cold-formed steel research and the developed design guidelines. CFS construction provides affordable, light, efficient, and resilient building systems. CFS members are obtained by forming thin steel sheets into several different cross-sections. Due to transportation, installation, and even production, geometrical imperfections may occur on the thin steel sheets that form the CFS members. These geometrical imperfections affect the predicted physical response of CFS members. Thus, in order to efficiently compute the physical response of a CFS member, it is necessary to determine the geometric imperfections and investigate their effect on the member behavior. In this paper, a low cost methodology for extracting the 3D surface data of CFS members from 2D images that could be later used for geometric imperfection extraction is proposed.

Introduction

CFS members diverge from the ideal as-design geometry due to various reasons. Geometric imperfections form due to these deviations from the ideal geometry and they are common in cold-formed steel members. Both strength and buckling behavior of CFS members are affected by the geometric imperfections. Thus, it is important to characterize these geometric imperfections and include their effects in the design in order to predict the behavior of these members accurately. However, the current methodologies used for extracting geometric imperfections involve collecting geometric data by using advanced 2D or 3D data collection equipment. Thus, it is necessary to develop an easy-to-use, low-cost solution.

In recent years, there have been several studies that focus on geometric imperfection measurement, extraction, and modeling. The influence of imperfections on the behavior of CFS members is investigated by Dubina and Ungureanu (2002). They also discussed the effects of the different types of local-sectional imperfections on the buckling resistance. Zeinoddini and Schafer (2011) measured the global imperfections and dimensional variations in CFS members. Certain imperfection types that are the global bow, camber, and twist are determined. The geometric imperfections that occur due to the manufacturing process are then investigated by Zeinoddini and Schafer (2012). Three approaches, which are Traditional Modal Approach, 2D Spectra Approach, and 1D Modal Spectra Approach, are used for simulating the imperfections. The 1D Modal Spectra Approach is found to be the most accurate approach for predicting the strength, axial flexibility, and failure mechanism of the members. The procedures for processing three-dimensional point clouds that are generated by laser scanning of CFS members in order to measure cross-section dimensions and extract imperfections, as well as to perform finite element simulations using the as-measured geometry, are discussed in Zhao et al. (2017). Selvaraj and Madhavan (2018) collected the surface data of 188 CFS members with varying cross-sectional geometries are collected with a 3D laser scanner and the related geometric imperfections are extracted. It was observed that the imperfections in the CFS members are in correlation with geometric properties such as slenderness ratios, torsional constant, and plate slenderness.

This paper focuses on developing a low cost method that enables 3D surface data extraction from 2D images. The surface data, which can also be referred to as point cloud, could then be used for geometric imperfection extraction in future studies. First, images of a CFS C-section mounted on a special test setup are collected. The collected images are then calibrated and enhanced for 3D surface data generation. The quality of the enhanced images is tested by performing keypoint extraction and matching. Finally, the quality controlled images are used for generating the surface mesh of the investigated CFS member.

Experiment

Title, authors, and authors' affiliations

The camera used in this study is a Nikon D7100 with a DX-format 23.5 mm x 15.6 mm CMOS image

DOI:10.35490/EC3.2019.181

sensor. In order to capture 2D images, this camera is positioned on a stationary tripod at a certain distance from the test setup. Each captured image consists of 24.1 Megapixels.

Cold-formed steel C-section

A C-sectioned CFS member is investigated in this study. In total 36 images, which cover the 360° around the member, are collected. The collected images are then converted into a surface mesh. In order to check the accuracy of the generated surface mesh, first, the actual dimensions of the CFS member are recorded with a micrometer. The measured dimensions are then compared with extracted dimensions. Figure 1 shows the locations from where the micrometer measurements are taken. Table 1 presents the measured dimensions related to the investigated CFS member. The extracted dimensions are presented in the following sections of the paper.

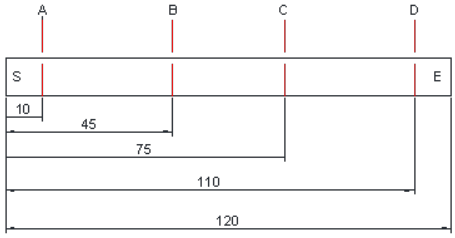

Figure 1: Measurement locations for dimension extraction of the C-section (dimensions are in cms).

Table 1: Dimensions of the C-section.

Measured Dimensions										
Point A					Point C				
Web Width (mm)		Flange Width (mm)	Lip Width (mm)		Web Width (mm)		Flange Width (mm)	Lip Width (mm)	
S1	S2	-	S1	S2	S1	S2	-	S1	S2
45.9	45.7	73.9	9.5	9.5	45.8	45.6	73.9	9.5	10.0
Point B					Point D				
Web Width (mm)		Flange Width (mm)	Lip Width (mm)		Web Width (mm)		Flange Width (mm)	Lip Width (mm)	
S1	S2	-	S1	S2	S1	S2	-	S1	S2
45.9	45.6	73.9	9.5	10.0	45.8	45.9	74.4	9.5	9.8

It should also be noted that since the original state of the investigated CFS member has a uniform and shiny surface texture, the surface the member is patterned. The pattern is generated by randomly spraying the surface of the member with a black dye from a distance of 1m. A permanent black dye suitable for metal surfaces is used. The generated surface pattern is later used for keypoint extraction and matching.

Test setup

Test setup consists of two plates attached to a ball-bearing. The plated located at the bottom is fixed and the plate on the top is free to rotate. There are 36 holes on the perimeter of the bottom plate, which are 10° apart from each other. On the top plate, however, there are only 4 holes. These 4 holes are used to secure the top plate on which the element is secured during image capturing process. 4 bars are placed in these holes and the bars are then inserted into the corresponding bottom plate holes.

There are one straight and two L shaped perforated plates located on the top plate. All the plates are free to move. The locations of the plates are determined based on the centroid of the investigated C-section. Once the CFS member is located on the top plate, the moving plates are positioned to secure the member in place.

The test setup is located in front of a white surface in order to generate contrast and a calibration sheet is attached to the white background. An image is recorded and the top plate is rotated 10°. This is repeated 36 times to collect 36 photos that cover the entire surface of the CFS member. Figure 2 presents the test setup on which a sample CFS member is attached from two different viewpoints.

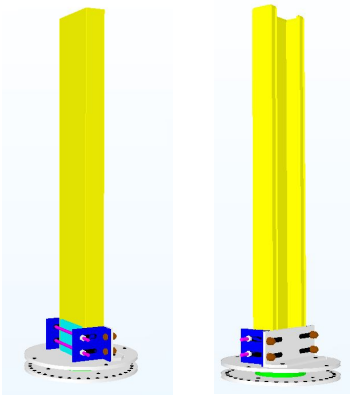

(a) (b)

Figure 2: Images of the test setup from two, (a) and (b), viewpoints.

Calibration and image enhancement

The collected images are calibrated as the first step of the surface mesh generation. To perform this, the Camera Calibrator application of MatLab (2018) is used. This application is capable of estimating the camera intrinsics, extrinsics, and lens distortion parameters. The obtained parameters are then used to remove the effects of lens distortion from the collected images. In this study, the known physical properties of the checkerboard image attached to the background are used for calibration. Figure 3 shows one of the calibrated images that belong to the collected 36 image set. The image contains the test setup, the attached CFS member, and the calibration paper.

The images are cropped to include only the test setup once the calibration process was completed. In order to crop the images to a certain size, the *imcrop* function of the MatLab is used. A location for a cropping rectangle is obtained from the first image and used on the rest of the 35 images.

Flash is not used during the image capturing due to the shiny surface of the CFS member, only cold light sources were used as additional lightening. As a result, the collected images are rather dark. In order to continue with further processing, it is required to enhance the quality of the images by making them more suitable for keypoint extraction. This requires increasing the contrast of the images. The images are first converted into grayscale images and the *imadjust* function of the MatLab is then used for adjusting image intensity values. The final image set is exported in *tiff* format. Figure 4 shows (a) a cropped image, (b) a grayscale image, and (c) an adjusted image.

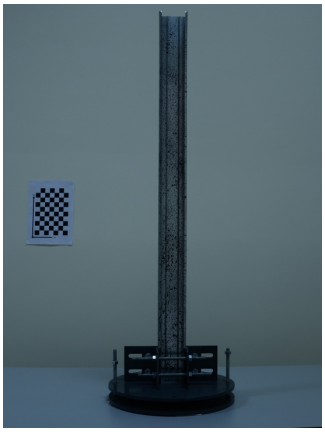

Figure 3: One of the calibrated 36 images that include the test setup, the attached CFS member, and the calibration paper attached to the wall behind.

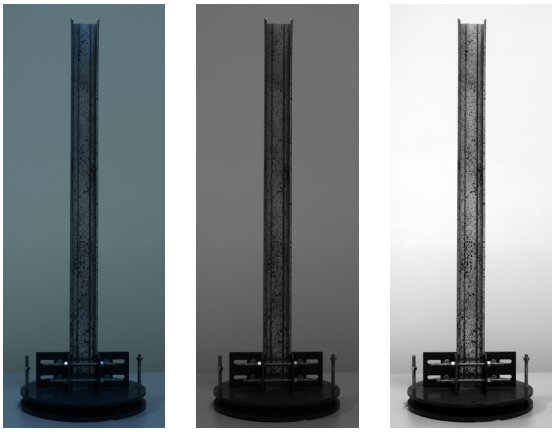

(a) (b) (c)

Figure 4: (a) Cropped image, (b) grayscale image, and (c) adjusted image.

Keypoint detection and matching for image quality verification

In this study, Regard3D (2018) is used for keypoint extraction and matching. This step is performed to ensure the quality of the enhanced images.

Regard3D (2018) is a structure-from-motion software that enables creating 3D models from objects using a series of photographs taken of an object from different viewpoints. For each image, keypoints that have a high probability of existence in a successive image are detected. Later, a mathematical descriptor based on local intensity order pattern is calculated for each keypoint. This descriptor has invariant characteristics that are present in successive images with different viewpoints. The descriptors from different images are matched and geometrically filtered. Figure 5(a) shows the keypoint detection results and Figure 5(b) shows the tracks in between the matched keypoints in two successive images. These results are used to confirm that the obtained images are sufficient for generating the 3D surface mesh of the investigated CFS member. The threshold for the number of keypoints for a successful match is taken as 8000.

(a) (b)

Figure 5: (a) Detected keypoints are shown on the member and (b) two successive images are matched based on the previously detected keypoints.

3D mesh generation

The next step of the method described in this paper is the surface mesh generation. This is achieved by using the Meshroom (2018) software. This software performs 3D surface mesh generation using overlapping 2D images collected from different viewpoints. Meshroom allows users to run a photogrammetric pipeline that starts with image insertion and ends with textured mesh generation.

The Meshroom software follows a 12 step analysis scheme. The first step of the process is feature extraction that is performed via scale-invariant feature transform. The aim is to extract discriminative patches in an image that can be compared to discriminative patches of a successive image irrespective of rotation, translation, and scale. Feature extraction is followed by image matching; the extracted features are matched by photometric matching. The software then runs the structure-from-motion algorithm. As an intermediary step; camera correction is performed automatically. The depth map extraction that is followed by depth map filtering is executed later. The software then performs meshing and mesh filtering. Finally, the generated surface mesh is covered with texture through texturing.

Figure 6 shows the end result of the mesh generation process. The surface mesh, which represents the CFS member, is in the middle of the screenshot. This surface mesh is surrounded with the camera locations from which the 36 images were captured. The camera locations are shown with white rectangles centered with white cubes.

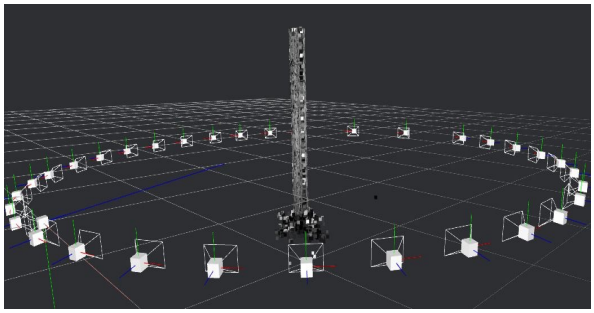

Figure 6: Generated mesh along with the camera poses for all of the 36 images used for processing.

3D mesh refinement

As the final step, MeshLab (2016) is used to improve the quality of the generated surface mesh and exclude the redundant regions. MeshLab is an open source system for processing and editing 3D triangular meshes. It provides a set of tools for editing, cleaning, healing, inspecting, rendering, texturing and converting meshes. Figure 7 presents the finalized surface meshes. Figure 7(a) and 7(b) show vertex presentations from two different perspectives that cover interior and exterior views. Figure 7(c) and 7(d) on the other hand represent smoothed surface meshes from two different perspectives that cover interior and exterior views.

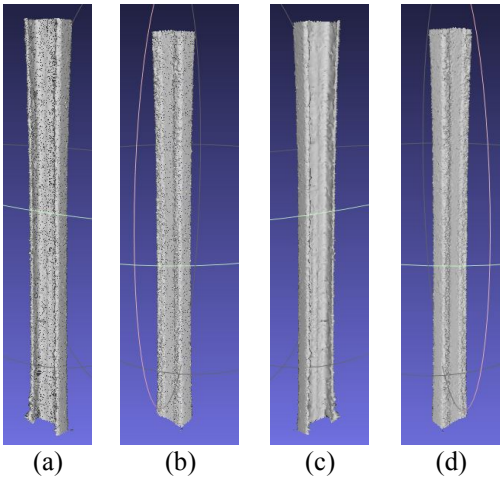

(a) (b) (c) (d)

Figure 7: Vertex representation for (a) interior and (b) exterior and smoothed surface mesh representation for (c) interior and (d) exterior.

Discussion and results

The accuracy of the generated surface mesh is verified by performing a dimension comparison between the micrometer measurements given in Table 1 and the dimensions extracted from the generated surface mesh. These dimensions are given in Table 2.

The surface mesh is then converted into a 3D point cloud in order to extract the necessary dimensions: web, flange, and lip. This point cloud is then used to extract the listed dimensions. However, it should be noted that it is not possible to extract lip dimensions from the generated point cloud due to noise. The error associated with the extracted web and flange dimensions is around 5%. Details of point cloud processing and dimension extraction can be found in Guldur (2014).

It should be noted that the accuracy of the generated 3D point cloud is directly related with the sensor used for image collection, the selected mesh generation algorithm, and the parameters chosen for meshing procedure.

Table 2: Dimensions extracted from the generated surface mesh.

Extracted Dimensions					
Point A			**Point C**		
Web Width (mm)		Flange Width (mm)	Web Width (mm)		Flange Width (mm)
S1	S2	-	S1	S2	-
48	49	74	47	48	74
Point B			**Point D**		
Web Width (mm)		Flange Width (mm)	Web Width (mm)		Flange Width (mm)
S1	S2	-	S1	S2	-
48	48	74	47	47	75

Conclusions

The geometric imperfections that occur on CFS members due to various reasons such as transportation, production, etc. could significantly change the physical response of the member. Thus, it is important to determine these imperfections and take their effect into account prior to construction.

This study focuses on developing a low cost methodology that uses 2D images to generate a 3D surface mesh by performing 3D image processing. The generated surface mesh is then used to extract the as-is dimensions of the investigated CFS member. It has been verified by the comparison of the measured vs. extracted member dimensions that the generated surface mesh is in good agreement with the as-is geometry of the investigated CFS member.

In future studies, the developed methodology will be tested on several CFS members and the generated surface mesh will be used to automatically extract geometric imperfections such as the bow, camber, etc.

Acknowledgments

This material is based upon work supported by the Scientific Research Projects Coordination Unit (BAP) of the Hacettepe University under Project No. FHD-2017-15248. Any opinions, findings and conclusions or recommendations expressed in this material are those of the authors and do not necessarily reflect the views of the Hacettepe University. The author would also like to thank Parkon Construction employees Omur Ozger, Emre Sakabas, and Ozerk Sazak for their support and guidance for the test setup design and production.

References

Dubina, D. & Ungureanu, V. (2002) Effect of Imperfections on Numerical Simulation of Instability Behaviour of Cold-Formed Steel Members. *Thin-Walled Structures,* 40**,** 239-262.

Guldur, B. 2014. *Laser-based Structural Sensing and Surface Damage Detection*. Ph.D. Dissertation, Northeastern University.

MatLab (2018) *MATLAB and Statistics Toolbox Release 2018b,* Natick, MA, The MathWorks, Inc.

MeshLab (2016) *MeshLab*, CNR.

Meshroom (2018) *Meshroom*, AliceVision.

Regard3D (2018) *Regard3D: A Structure-from-motion Program*, Regard3D.

Selvaraj, S. & Madhavan, M. (2018) Geometric Imperfection Measurements and Validations on Cold-Formed Steel Channels Using 3D Noncontact Laser Scanner. *Journal of Structural Engineering,* 144.

Zeinoddini, V. & Schafer, B. (2012) Simulation Of Geometric Imperfections in Cold-Formed Steel Members using Spectral Representation Approach. *Thin-Walled Structures,* 60**,** 105-117.

Zeinoddini, V. & Schafer, B. W. (2011) Global Imperfections and Dimensional Variations in Cold-Formed Steel Members. *International Journal of Structural Stability and Dynamics,* 11**,** 829-854.

Zhao, X., Tootkaboni, M. & Schafer, B. W. (2017) Laser-Based Cross-Section Measurement of Cold-Formed Steel Members: Model Reconstruction and Application. *Thin-Walled Structures,* 120**,** 70-80.